A continuum damage model for alveolar bone remodeling

M. Mengoni and J.P. Ponthot

Department of Aerospace and Mechanics, University of Liège

B52/3 - Chemin des chevreuils, 1 - 4000 Liège Belgium

e-mails: {*mmengoni, jp.ponthot*}*@ulg.ac.be*

Abstract

Several authors ([1, 2] among others) have proposed mechanical models to predict long term tooth movement considering both the tooth and its surrounding bone tissue as isotropic linear elastic materials coupled to an "adaptative elasticity" behavior [3, 4]. However, tooth movements obtained through orthodontic appliances result from a complex biochemical process of bone structure and density adaptation to its mechanical environment, called bone remodeling. This process is far from linear elasticity. It leads to permanent deformation due to biochemical actions. The proposed biomechanical constitutive law (inspired from Doblaré's model [5]) is based on a Continuum Damage Mechanics material coupled to an elasto-visco-plastic law and considering a damage variable not as actual damage but as a measure of bone density. It is formulated as to be used explicitly for alveolar bone, whose remodeling cells, opposite to most bones, are triggered by the pressure state applied to the bone matrix.

1 Introduction

One of the guiding principle in orthodontics is to gradually impose progressive and irreversible bone deformations. These modifications are due to bone remodeling, a biochemical process of skeletal adaptation to applied loads, mechanically controlled by bone cells. By optimizing load positions and intensities, treatment can be reduced both in time and cost. This optimization requires a mechanical model of the biochemical phenomena present activated dental movement. The goal of this work is to provide a constitutive model able to simulate those coupled phenomena.

For most type of bones [6, 7, 8], the physiological remodeling process takes place in order to adjust the amount of tissue and its topology according to long term loading conditions, following what is called "Wolff's law" of bone adaptation. Bone resorption occurs when disuse is observed. This resorption tends to decrease the amount of bone when it is not mechanically loaded. Bone apposition occurs in overloaded conditions, in order to reinforce bone where it is necessary. The bone therefore adapts its density in such a way to achieve an homeostatic state of stresses. Besides the density change, remodeling also occurs to change the bone topology, mainly in trabecular bone for which the trabeculae tend to align along the stress principal directions. A well known example can be observed on the human femur. The trabecular architecture of its proximal end, when loaded transversally at its cantilever end, resemble the principle stress trajectories of a Cullman crane with the same loading conditions, see [9] among others for a visual description.

Contrary to the majority of bones, alveolar bone remodeling seems on a macroscopic scale to depend mainly on the pressure state [10, 11, 12]. One can observe apposition on the tension side of a tooth when loaded with an abnormal mechanical environment, such as the one obtained with orthodontics appliances, as well as resorption on the compression side. The actual mechanical stimulus for such a difference is not quite clear and uniform among biology and biochemistry literature (see among others [8, 13, 14]). Some works focus on the periodontal ligament (PdL), a complex membrane of high vascularity seated between the teeth and the bone, non linear response (see among others [10, 15, 16, 17, 18, 19]). Its non linearity and different behavior in traction and compression leads to opposite loading conditions

of the bone on each side of the tooth. The compressive side of the tooth would lead to underuse of the bone and therefore resorption while the traction side would lead to overuse and apposition. However, when no non-linearities are considered in the PdL, no difference in the stress level can be observed.

Instead of focusing on the PdL response, the present work concentrates on the bone behavior during remodeling. We assume the pressure state (positive or negative) of the bone matrix as the key stimulus to differentiate apposition and resorption in overloaded conditions. This can be justified as follows. The cell supply needed for bone remodeling is performed by the vasculature, however, the alveolar bone main cell supply is through the periodontal ligament. As this membrane's stiffness is much less than the surrounding tissue's, the strain level is high. If the hydrostatic stress level is higher than the blood vessels' internal pressure, the blood flow is stopped as well as the remodeling cell supply to the bone. The remodeling process is therefore triggered by PdL pressure and stopped when these stresses are too high. We therefore assume that it is the same stimulus which is responsible for the differentiation between apposition and resorption and for the triggering of the phenomenon.

Within the diverse approaches that have been adopted to model bone remodeling processes, most of them are qualified as phenomenological models. They are models that do not try to predict the evolution of the microstructure and biological constitution of a tissue or an organ as a consequence of the mechanical environment (contrary to Mechanobiological models) but whose goal is to predict the mechanical behavior (movement, strains and stresses) of a tissue or an organ, taking into account the applied loads, its microstructure and the constraints imposed by other organs. Most of these models admit the existence of a certain mechanical stimulus (input) that produces bone apposition or resorption (output) in such a way that the stimulus tends to a certain physiological level in the long-term (homeostasis). Among these phenomenological models, the definition of a remodeling stimulus uses a wide range of mechanical measures : stresses, strains, strain energy density, strain rate or even damage. The model which is proposed in this work is built on a damage/repair based model stated first by Doblaré and co-workers [5, 20, 21]. This model has been chosen as a working base because it is one of the few models whose stimulus variation is justified through thermodynamical concepts of continuum mechanics. It is here extended in order to be used for the alveolar bone and therefore it takes into consideration the pressure state of the tissue as one of the stimulus for bone remodeling. It is also coupled to an elasto-visco-plastic material behavior in order to capture permanent strains of the tissue.

2 Material and Methods

Based on previous works, Beaupré, Carter and co-workers [22, 23, 24, 25] developed a model (called the Stanford model) considering that bone tissue needs a certain level of mechanical stimulus to maintain homeostasis and auto-regulates itself to maintain such a level. Their objective is to homogenize a local mechanical stimulus (ψ, a daily stress stimulus at tissue level) in values near an homeostatic level ($\psi^\star$). The density variation ($\dot{\rho}$, Eq.(1)) is then proportional to a remodeling rate ($\dot{r}$), a non linear function of the mechanical stimulus error ($\psi - \psi^\star$) as well as to the specific surface S_v described by Eq.(7).

$$\dot{\rho} = k S_v \rho_0 \, \dot{r}(\psi - \psi^\star) \tag{1}$$

The remodeling rate also takes into consideration the existence of a lazy zone (width of 2Ω) within which no remodeling is achieved (Figure 1). The actual existence of this lazy zone is again a concept which is not uniformly accepted among the biological community. Some people do seem to believe that this zone has been introduced by the numerical community for convergence purpose more than for actual biological reasons.

Once the density variation is computed, an "adaptative elasticity" approach [3, 4] is performed : the bone Young's modulus is updated following the density update using a law such as :

$$E = \begin{cases} 2014\,\rho^{2.5}\,[MPa] & : \text{ if } \rho \leq 1.2\ g/cc \\ 1763\,\rho^{3.2}\,[MPa] & : \text{ if } \rho \geq 1.2\ g/cc \end{cases} \tag{2}$$

$$\text{In general :} \qquad E = B(\rho)\rho^{\beta(\rho)} \tag{3}$$

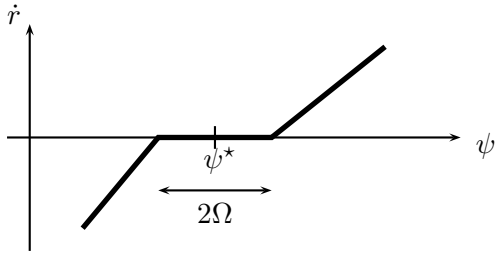

Figure 1: Stanford remodeling rate

Doblaré and co-workers [5, 20, 21] adapted this model so as to formulate it in a Continuum Damage Mechanics approach [26, 27], see appendix 1 for an overview of the principles. They consider an anisotropic damage coupled to a linear elastic material (in the case of isotropy, the damage variable can be written : $d = 1 - E/E_0$). The undamaged material is considered as the ideal situation of bone with null porosity and perfect isotropy. The process of bone resorption corresponds to the classical damage evolution concept, since it increases the porosity (decreases the density). On the other hand, it should be emphasized that bone apposition can produce damage reduction or bone repair.

Using a continuum damage approach as well as Eq.(2), one can get for both types of bone (trabecular and cortical bones), using $\rho_0 = 2.1 g/cc$ (and therefore $E_0 = 18.9 GPa$) for the fully mineralized bone :

	Density[a]		Stiffness	Damage[b]	Porosity[c]
	$\rho[g/cc]$		$E[GPa]$	d	f
Trabecular bone	1.15	$\rightarrow$	2.9	0.85	0.45
Cortical bone	1.99	$\rightarrow$	16.1	0.15	0.05

[a] Arbitrary values are presented

[b] Damage is calculated from stiffness as : $d = 1 - \dfrac{E}{E_0}$

[c] Porosity is calculated from density as : $f = 1 - \dfrac{\rho}{\rho_0}$

Table 1: Bone stiffness, damage and porosity as a function of density, for an isotropic material

In analogy with plasticity, a remodeling stimulus is identified with the variable thermodynamically associated with damage. Doblaré and co-workers therefore establish two damage criteria, g_f and g_r (Eq.(4) in their isotropic formulation), representing the domain of the remodeling stimulus for which damage is not modified (the lazy zone) both for resorption and formation. These criteria depend on U, function of a strain energy density as well as the density and the number of cycles considered for the applied loads, and $U^\star$, a reference homeostatic value of U. They are consistent with Beaupré and Carter's approach if we relate ψ to U, $\psi^\star$ to $U^\star$ and Ω to ω, the normalized width of the lazy zone (as done in appendix 2).

$$\left\{ \begin{array}{rcl} g_f & = & U - U^\star(1+\omega) < 0 \\ g_r & = & 1/U - 1/(U^\star(1-\omega)) < 0 \end{array} \right. \tag{4}$$

Using consistency conditions and Eq.(1) of the Stanford model, they can explicit the damage variation (Eq.(5) in its isotropic formulation, the proportionality constant being different for bone resorption and bone apposition) as proportional to a remodeling rate such as the one proposed by the Stanford group and presented on Figure 1.

$$\dot{d} \propto -k S_v \dot{r} \tag{5}$$

As stated previously in this paper, this type of bone remodeling model cannot be applied to alveolar bone if no PdL nonlinearities are considered. We propose a model that uses an approach similar to Doblaré's one, both for the damage definition and variation and the damage criteria. However, in accordance to the observation of a pressure dependent phenomenon, the remodeling rate definition is modified (Figure 2, Eq.(6)) taking into account the pressure state.

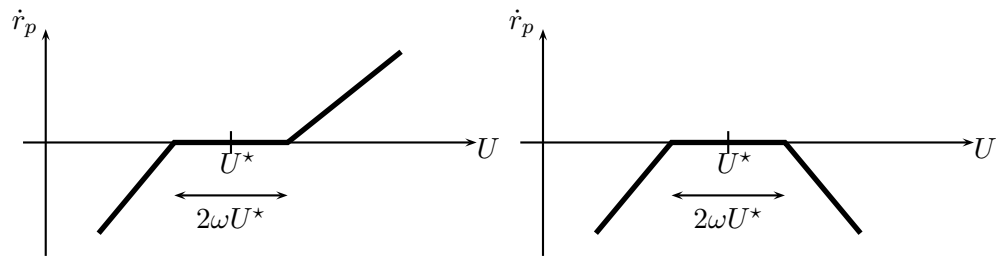

(a) $p > 0$ (b) $p < 0$

Figure 2: Pressure dependent remodeling rate, pressure p being positive in traction.

$$\dot{r}_p = \begin{cases} c_f \dfrac{g_f}{\rho^{2-\beta/2}} & \text{if } g_f \geq 0,\ g_r < 0 \quad \text{and} \quad p > 0 \\ -c_r \dfrac{g_f}{\rho^{2-\beta/2}} & \text{if } g_f \geq 0,\ g_r < 0 \quad \text{and} \quad p < 0 \\ -c_r \dfrac{g_r}{\rho^{2-\beta/2}} & \text{if } g_r \geq 0,\ g_f < 0 \\ 0 & \text{if } g_f < 0,\ g_r < 0 \end{cases} \tag{6}$$

Where c_r and c_f are two remodeling constants, β the density related parameter introduced in Eq(3) and p , the pressure, positive in traction.

The damage used is virtual and is a measure of bone density. There is no actual damage in the tissue. The damage evolution is proportional to the defined remodeling rate so that repair will occur in the case of tissue formation, for overloaded traction conditions. Damage will increase in the case of tissue resorption, both in the case of overloaded compression conditions and underloaded conditions.

As stated earlier, the damage evolution is proportional to the specific surface, S_v as defined by [28]. It is written as a 5th order polynomial of the porosity and is null for null porosity as well as for full porosity ($f = 1.0$).

$$S_v = 28.5f^5 - 101.1f^4 + 133.7f^3 - 93.1f^2 + 32f \tag{7}$$

This specific surface is introduced in order to take into account the necessity of a bone surface to exist for bone remodeling cells to act. When the porosity is close to 0.0 or 1.0 (see Figure 3), the available surface for bone remodeling is close to 0.0 while for intermediate porosities, this surface reaches a maximum. Its presence in the damage variation law has therefore a biological justification but also serves a numerical purpose. Using this specific surface will decrease substantially the convergence

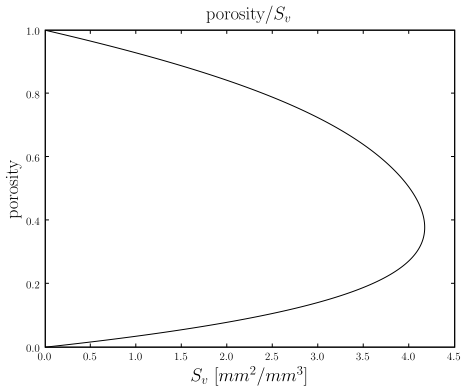

Figure 3: Specific surface variation with porosity value

problem that would arise when reaching high damage values. Indeed, the effective stress definition of the continuum damage theory in a strain equivalence approach can be written for an isotropic damage

variable, d, as

$$\tilde{\boldsymbol{\sigma}} = \frac{\boldsymbol{\sigma}}{1-d} \tag{8}$$

Therefore when obtaining a damage variable close to 1.0 (full resorption of the bone), the model cannot be used anymore. Yet, this will tend not to happen in the model because when reaching the critical value, the damage variation decreases substantially and the tendency to reach the critical value (for which the damage variation is null) is reduced. However, it also has to be noticed that for an initial null bone porosity, there will be no damage apparition, because of the zero value of the specific surface at that point. This would mean that a fully mineralized bone could not be resorbed.

Opposite to Doblaré's approach, this continuum damage model is coupled to a visco-plastic material behavior. One can therefore consider permanent deformation of the bone as a process due to both permanent strain (and therefore plasticity-like, although it is clear that the relevant inelastic process is different from that of the classical metal plasticity) and change in bone density. It can also be used to describe a fracture process with a plasticity-like yield function to model the envelope of bone failure.

Once the remodeling model has been formulated, we need to check its ability to achieve qualitative results close to the ones obtained in experimental tests of actual alveolar bone. This is accomplished in the next section in which the model is applied to the study of the remodeling behavior of the alveolar bone in the case of orthodontics treatments.

3 Numerical results

In this section, we consider the potential of this pressure dependent model to predict the density evolution of bone tissues. As an example, we present a 2D model of a tooth surrounded by its parodontal tissue, on the crown of which a pressure load is applied in the vestibulo-lingual direction. The aim is to predict the bone density and its evolution from an initial ideal situation (isotropic material with uniform density distribution) when loaded by forces that characterize the orthodontics appliances. Neither this problem nor the starting situation are "real" problems, therefore, the homeostatic values are not relevant (as well as the other parameters of the model, especially for a qualitative evaluation). The tooth geometry is idealized, with a parabolic root surrounded by a constant thickness periodontal ligament as well as trabecular and cortical bone. The 2D discretization used here is shown in Figure 4. The root is $12mm$ high and $6mm$ wide at the collar. The crown is $7mm$ high, the PdL's thickness is constant and of $0.2mm$. It is surrounded by a trabecular bone of variable thickness and a cortical layer of around $0.5mm$ width. The tooth and the PdL mechanical behavior is elastic ($E_{\text{tooth}} \approx 20GPa$, $\nu_{\text{tooth}} = 0.3$, $E_{\text{PdL}} = 0.6MPa$, $\nu_{\text{PdL}} = 0.45$). The cortical layer as well as the trabecular bone mechanical behavior is elasto-plastic with a continuum damage model (elasticity parameters as in Table 1). The damage evolution follows the remodeling law proposed in this work. Finite Element analysis is performed, using large strains

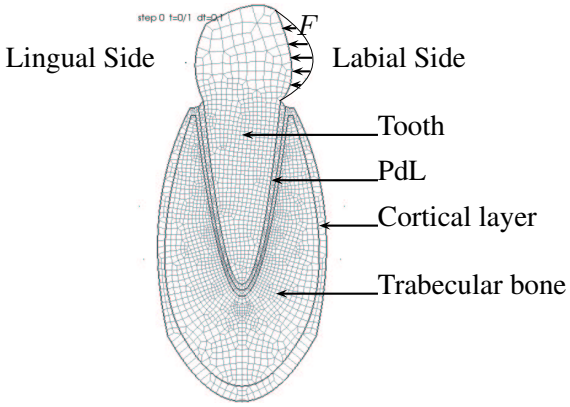

Figure 4: Tooth and surrounding tissue - mesh and geometry

code METAFOR [29], considering a plane strain state as well as a quasi-static analysis. The basal bone junction is restrained in both vertical and horizontal directions. The mesh is composed of 2670 nodes and 2600 linear quadrangular elements. Loading is performed using two levels of pressure value (corresponding to $1.0N$ and $2.0N$ force) as well a as different sets of remodeling constants (see Table 2).

Force	$c_r = c_f$ $[\mu m/day]$	c_r, c_f $[\mu m/day]$
(case 1) : 1N	2.0	1.0, 4.5
(case 2) : 2N	1.0	0.5, 2.25

Table 2: Remodeling constants used for trabecular bone

The obtained tooth movement is a rotation around a center of rotation situated at one third of the root length starting from the apex for small loads and one fifth for higher loads. The rotation angle is almost null for small forces, corresponding to initial tooth mobility, while it reaches about 1.5 degrees for higher forces. The initial tooth mobility depends only on the applied load and not on the remodeling model used. However the possibilities of long term tooth movement due to bone density change varies strongly with the type of model used (1 constant or 2 constants model) as well as with the homeostatic value $\psi^\star$ and the number of cycle considered.

When using the same remodeling constant for both resorption and formation, one does not exactly gets symmetric values for damage variation (Figure 5, top row) because of its dependence on the damage value (damage variation increases while damage decreases). In the case of two different remodeling constants (Figure 5, bottom row), the one used in resorption, c_r, is the restrictive one because it is the one increasing the damage value. Its value is restrained so that the damage value cannot reach 1.0. The constant used in formation, c_f, can be increased almost at will (as long as numerical convergence is concerned, not from a biological point of view). However, if too high, the effective stiffness will increase, so will the stress. The stress state around the apex will be modified and affect the resorption side as well (with a tendency to increase the resorption). Concerning the stress state of the periodontal ligament, it

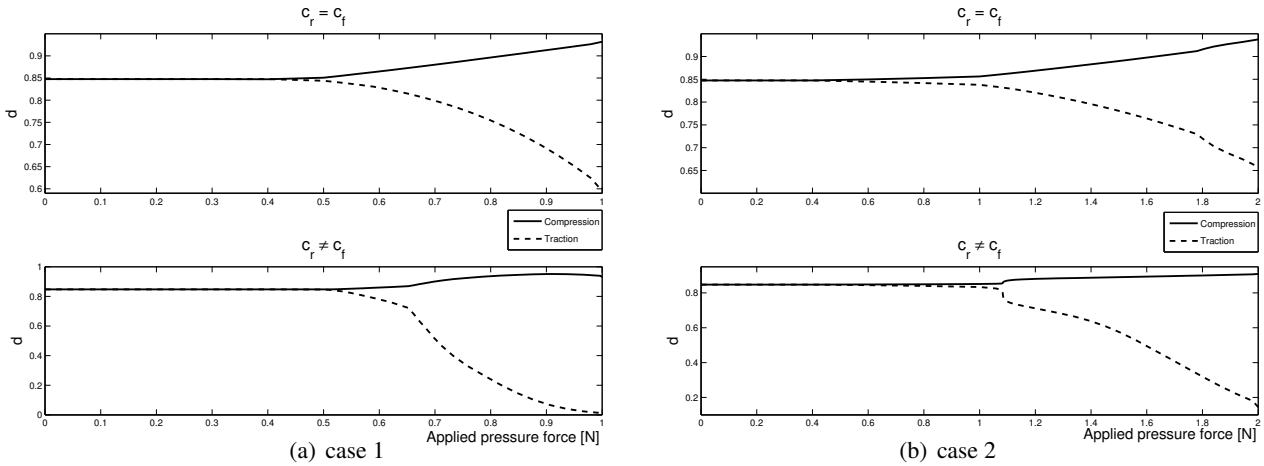

(a) case 1 (b) case 2

Figure 5: Damage variation at the apex for a pressure dependent model - both for the compression side for which c_r is used (plain line) and the traction one for which c_f is used (dashed line).

is interesting to notice that the hydrostatic stresses are several times higher than the shear stresses (up to 8 times for low forces). For the lower applied load, the later ones vary from 0 to $0.025MPa$ along the tooth root (highest values reached at the collar) while the hydrostatic stresses'range goes from 0 to $0.2MPa$ both in compression and traction (highest values reached at the level of the center of rotation position). The pressure is as expected the key stress in the PdL.

Qualitatively analyzing the results of this model, one can see (as in figures 6 and 7), as can be expected of an orthodontic treatment, that while higher loads lead to higher initial displacement, density variation of the bone can be observed only in the apex region while it is observed on the entire length of the root for smaller loads. As the remodeling law has been built so, one can see that the bone gets resorbed on the compression side and formed on the traction one along the root but also along the cortical layer when high displacements are obtained (as on figures 6-(c) and 7-(c)).

4 Discussion

The present study introduced a numerical model for the simulation of orthodontic tooth movement based on the assumption that bone remodeling processes during tooth movement are controlled by elastic energy density as well as pressure state of the alveolar bone. In spite of the necessary idealizations, a reliable qualitative prediction of bone density variation around the tooth is possible for porosities variations from 0% (null damage) to almost 70% (damage of 0.95), starting from an homogenized porosity of 45%.

Next investigations will have to focus on the functional description of the orthodontic "remodeling law". So far anisotropic phenomena cannot be considered while bone's intrinsic anisotropy leads to remodeling processes directionality dependent. The simulation presented allows a prediction of tooth movement's initiation. It should be completed by long term tooth movement issues such as actual bone loss and creation with fracture-like criteria for loss or creation of elements.

References

[1] J. Schneider, M. Geiger, and F.-G. Sander. Numerical experiments on long-time orthodontic tooth movement. *American Journal of Orthodontics and Dentofacial Orthopedics*, 121(3):257–265, Mar 2002.

[2] G.-Q. Song. Three dimensional finite element stress analysis of post-core restored endodontically treated teeth. Master's thesis, Universtity of Manitoba (Canada), 2005.

[3] S. C. Cowin and D. H. Hegedus. Bone remodeling i: theory of adaptive elasticity. *Journal of Elasticity*, V6(3):313–326, July 1976.

[4] D. H. Hegedus and S. C. Cowin. Bone remodeling ii: small strain adaptive elasticity. *Journal of Elasticity*, V6(4):337–352, October 1976.

[5] M. Doblaré and J. M. García. Anisotropic bone remodelling model based on a continuum damage-repair theory. *J Biomech*, 35(1):1–17, Jan 2002.

[6] S. C. Cowin. Tissue growth and remodeling. *Annu Rev Biomed Eng*, 6:77–107, 2004.

[7] W. E. Roberts. Bone physiology of tooth movement, ankylosis, and osseointegration. Seminars in Orthodontics, 2000. Volume 6, Issue 3, September 2000, Pages 173-182.

[8] W. E. Roberts, S. Huja, and J. A. Roberts. Bone modeling: biomechanics, molecular mechanisms, and clinical perspectives. Seminars in Orthodontics, 2004. Volume 10, Issue 2, June 2004, Pages 123-161.

[9] S. C. Cowin and S. B. Doty. *Tissue Mechanics*. Ed. Springer, 2007. Ch. 11 : Bone tissue.

[10] C. Bourauel, D. Freudenreich, D. Vollmer, D. Kobe, D. Drescher, and A. Jäger. Simulation of orthodontic tooth movements. a comparison of numerical models. *J Orofac Orthop*, 60(2):136–151, 1999.

[11] C. Bourauel, D. Vollmer, and A. Jäger. Application of bone remodeling theories in the simulation of orthodontic tooth movements. *J Orofac Orthop*, 61(4):266–279, 2000.

[12] B. Melsen. Tissue reaction to orthodontic tooth movement–a new paradigm. *Eur J Orthod*, 23(6):671–681, Dec 2001.

[13] R. S. Masella and M. Meister. Current concepts in the biology of orthodontic tooth movement. *American Journal of Orthodontics and Dentofacial Orthopedics*, 129(4):458–468, Apr 2006.

[14] V. Krishnan and Z. Davidovitch. Cellular, molecular, and tissue-level reactions to orthodontic force. *American Journal of Orthodontics and Dentofacial Orthopedics*, 129(4):469.e1–469.32, Apr 2006.

[15] M. Cronau, D. Ihlow, D. Kubein-Meesenburg, J. Fanghänel, H. Dathe, and H. Nägerl. Biomechanical features of the periodontium: an experimental pilot study in vivo. *American Journal of Orthodontics and Dentofacial Orthopedics*, 129(5):599.e13–599.e21, May 2006.

[16] J. Middleton, M. Jones, and A. Wilson. The role of the periodontal ligament in bone modeling: the initial development of a time-dependent finite element model. *American Journal of Orthodontics and Dentofacial Orthopedics*, 109(2):155–162, Feb 1996.

[17] C. Verna, M. Dalstra, T. Clive Lee, P. M. Cattaneo, and B. Melsen. Microcracks in the alveolar bone following orthodontic tooth movement: a morphological and morphometric study. *Eur J Orthod*, 26(5):459–467, Oct 2004.

[18] C. G. Provatidis. A comparative fem-study of tooth mobility using isotropic and anisotropic models of the periodontal ligament. finite element method. *Med Eng Phys*, 22(5):359–370, Jun 2000.

[19] A. Natali, editor. *Dental Biomechanics*. Taylor and Francis, 2003.

[20] J. M. García, M. Doblaré, and J. Cegonino. Bone remodelling simulation: a tool for implant design. *Computational Materials Science*, 25(1-2):100–114, September 2002.

[21] T. Rüberg. Computer simulation of adaptive bone remodeling. Master's thesis, Technische Universität Braunschweig Centro Polictécnico Superior Zaragoza - Germany, 2003.

[22] G. S. Beaupré, T. E. Orr, and D. R. Carter. An approach for time-dependent bone modeling and remodeling–theoretical development. *J Orthop Res*, 8(5):651–661, Sep 1990.

[23] G. S. Beaupré, T. E. Orr, and D. R. Carter. An approach for time-dependent bone modeling and remodeling-application: a preliminary remodeling simulation. *J Orthop Res*, 8(5):662–670, Sep 1990.

[24] C. J. Hernandez, G. S. Beaupré, T. S. Keller, and D. R. Carter. The influence of bone volume fraction and ash fraction on bone strength and modulus. *Bone*, 29(1):74–78, Jul 2001.

[25] C. R. Jacobs, J. C. Simo, G. S. Beaupre, and D. R. Carter. Adaptive bone remodeling incorporating simultaneous density and anisotropy considerations. *Journal of Biomechanics*, 30(6):603–613, June 1997.

[26] J.-L. Chaboche. *Description thermodynamique et phénoménologique de la viscoplasticité cyclique avec endommagement.* PhD thesis, Université Pierre et Marie Curie,Paris VI, 1978.

[27] J. Lemaitre and R. Desmorat. *Engineering Damage Mechanics: Ductile, Creep, Fatigue and Brittle Failures*. Springer, 2005.

[28] R.B. Martin. Porosity and specific surface of bone. *Crit Rev Biomed Eng*, 10(3):179–222, 1984.

[29] Metafor : a large strain finite element code. http://garfield.ltas.ulg.ac.be/dokuwiki/metafor.

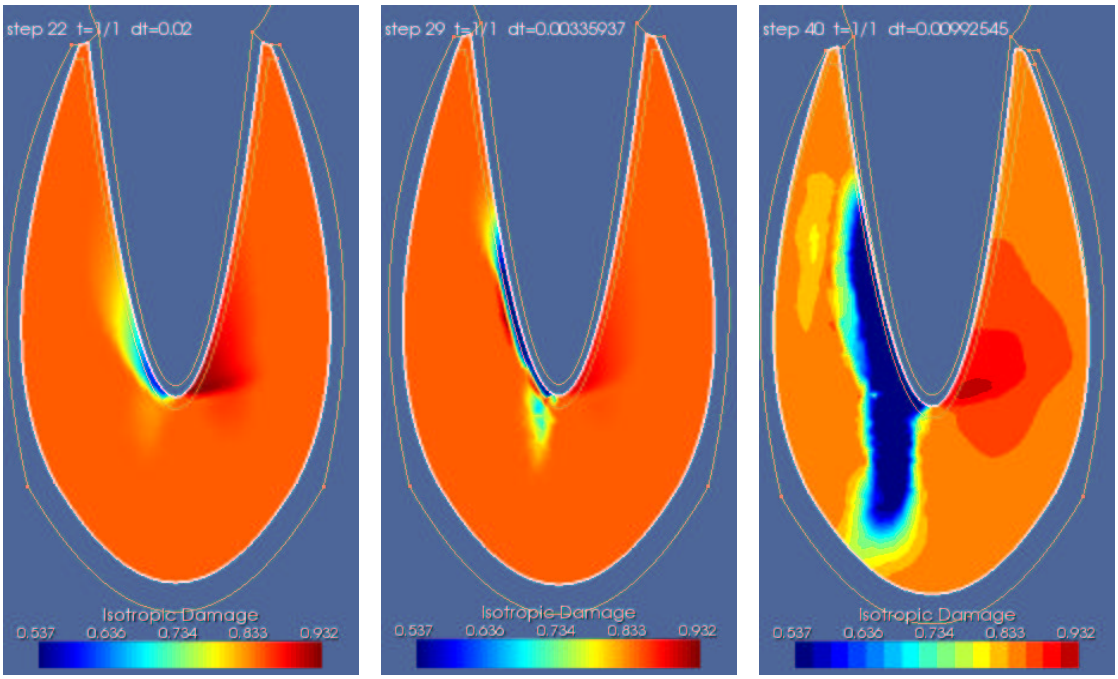

(a) (b) (c)

Figure 6: Alveolar bone damage - (a) case 1, $c_r = c_f$ - (b) case 1, $c_r \neq c_f$ - (c) case 2, $c_r \neq c_f$. For comparison purpose, damage interval has been set from .54 to .93 but lowers to 0.0 in case (b) and varies from .13 to .91 in case (c) as shown on Figure 7.

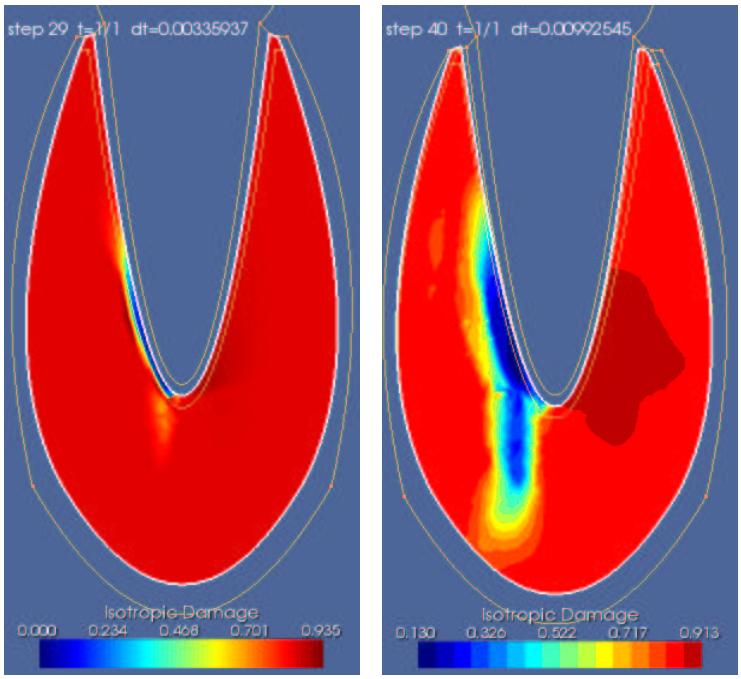

(b) (c)

Figure 7: Alveolar bone damage - zooming on Figure 6-(b) and (c)

Appendix 1 : Continuum Damage Principles

Continuum Damage Mechanics is a theory first presented by Chaboche in 1978 [26, 27]. It is a macroscopic description of damage. It uses the concept of effective stress, the stress acting to the actual surface area resisting the applied force. For isotropic damage, it can be written as Eq.(8). Using the strain equivalence approach, relating the stress level in the damaged material with the stress in the undamaged material that leads to the same strain, one can write for an elastic material :

$$\tilde{\boldsymbol{\sigma}} = \mathbb{C} : \boldsymbol{\varepsilon} \tag{a}$$

where $\tilde{\boldsymbol{\sigma}}$ is the effective stress as defined on equation 8, $\mathbb{C}$ is Hooke's fourth order elasticity tensor and $\boldsymbol{\varepsilon}$ the strain tensor.

Doblaré's model is actually written using the strain energy density equivalence approach getting the same strain energy density in the damaged and undamaged material by the definition of an equivalent stress and an equivalent strain. The elasticity law is therefore written : $\tilde{\boldsymbol{\sigma}} = \mathbb{C} : \tilde{\boldsymbol{\varepsilon}}$. One can switch from one representation to the other by changing the damage definition. For the strain energy equivalence approach, isotropic damage is defined as $d = 1 - \sqrt{\frac{E}{E_0}}$ instead of $d = 1 - \frac{E}{E_0}$ in a strain equivalence approach. However, in order to be compatible with the already existing continuum damage material model in METAFOR [29], a strain equivalence approach is used in this work.

Eq.(a) can be used in the case of an elasto-visco-plastic material (using an objective time derivative and considering an additive decomposition of the strain rate : $\dot{\boldsymbol{\varepsilon}} = \dot{\boldsymbol{\varepsilon}}^{el} + \dot{\boldsymbol{\varepsilon}}^{vpl}$) and becomes (with no time variation of $\mathbb{C}$) :

$$\dot{\tilde{\boldsymbol{\sigma}}} = \mathbb{C} : \dot{\boldsymbol{\varepsilon}}^{el} = \mathbb{C} : \dot{\boldsymbol{\varepsilon}} - \mathbb{C} : \dot{\boldsymbol{\varepsilon}}^{vpl} \tag{b}$$

where $\dot{\boldsymbol{\varepsilon}}^{vpl}$ can be calculated from the normality rule on the yield surface with an iterative integration process.

Appendix 2 : Relation between Doblaré's and Stanford's stimulus

One can relate Doblaré and co-workers'model to Stanford's if noticing that the first one is adapted from the later according to the density level :

$$\begin{aligned} U &\propto \rho_0^{2-\beta/8} A^{1/8} \sqrt{\bar{u} B} \\ \psi &\propto \bar{u} \\ U^\star &= \psi^\star \rho^{2-5\beta/8} \\ \omega &= \Omega/\psi^\star \end{aligned}$$

where β and B are defined in Eq.(3), $A = \dfrac{B}{B_0}\rho_0^{\beta-\beta_0}$ and $\bar{u}$ is the effective elastic energy density (as also defined by [27]):

$$\bar{u} = \int \tilde{\boldsymbol{\sigma}} : d\boldsymbol{\varepsilon}^{el} = \frac{\tilde{J}_2^2}{2E}\left[\frac{2}{3}(1+\nu) + 3(1-2\nu)\frac{\tilde{p}^2}{\tilde{J}_2^2}\right]$$

According to B, β and $\bar{u}$ dimensions, $\psi^\star$ is of stress dimension and is therefore a good candidate for a stress level measurement.